THE JOURNAL OF PHYSICAL CHEMISTRY A

Article

pubs.acs.org/JPCA

Reactions of Criegee Intermediates with Alcohols at Air−Aqueous Interfaces

Shinichi Enami*,† and A. J. Colussi*,‡

†National Institute for Environmental Studies, 16-2 Onogawa, Tsukuba, Ibaraki 305-8506, Japan

‡Linde Center for Global Environmental Science, California Institute of Technology, Pasadena, California 91125, United States

Supporting Information

ABSTRACT: The fate of Criegee intermediates (CIs) from the gas-phase ozonolysis of unsaturated organic compounds in the troposphere is largely controlled by their reactions with water vapor. We recently found that against all expectations carboxylic acids compete at millimolar concentrations with water for CIs at the air−liquid interface of aqueous organic media. This outcome is consistent with both the low water concentration in the outermost interfacial layers and the enrichment of the competing acids therein. Here we show, via online electrospray mass spectrometric detection, that CIs generated in situ in the fast ozonolysis of sesquiterpenes ($C_{15}H_{24}$) on the surface of water:acetonitrile microjets react with $n \geq 4$ linear alcohols $C_nH_{2n+1}OH$ to produce high molecular weight C_{15+n} ethers in one step. The OH group of 1-octanol proved to be ∼25 times less reactive than that of *n*-octanoic toward CIs at the same bulk molar concentration, revealing that the reactivity of hydroxylic species depends on both acidities and interfacial affinities. CI interfacial reactions with surface-active hydroxylic species, by bypassing water, represent shortcuts to molecular complexity in atmospheric aerosols.

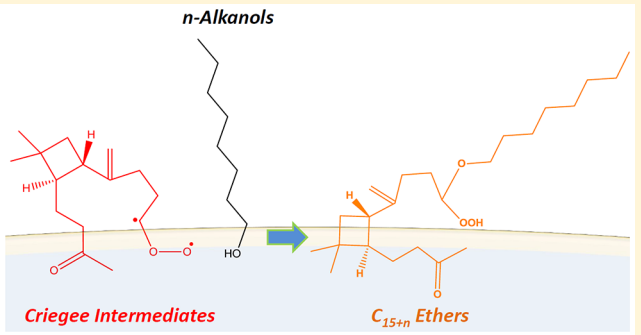

INTRODUCTION

Ozonolysis of unsaturated hydrocarbons (such as those from massive biogenic terpene emissions) is the leading source of Criegee intermediates (CIs)[1] in the atmosphere. CIs have a major role in atmospheric HO_x cycling and in particle formation, particularly over forests.[2−11] Unsaturated hydrocarbons are also deemed to be reactively uptaken on the surface of acidic aerosols and leaf films,[12−14] where they would react with O_3(g) to generate CIs in situ.[15,16] The fate of the CIs generated on the surface of aqueous organic aerosols, however, is not known. Theoretical calculations predicted that the reaction of the smallest CI (CH_2OO) with water molecules at the air−water interface would proceed ∼10^2 to 10^3 faster than in the gas phase.[17] In this regard, we recently found that in the outermost interfacial layers of water/acetonitrile mixtures, as surrogates of aqueous organic aerosol media, long-chain carboxylic acids at millimolar concentrations compete with $(H_2O)_n$ for CIs.[18] We ascribed this finding to the low water concentrations prevalent in the outermost interfacial layers of such mixtures, and to the surface enrichment of the more hydrophobic carboxylic acids. We also found that surface-active *cis*-pinonic acid (CPA), a major product of the ozonolysis of biogenic monoterpenes, is a particularly reactive scavenger of CIs on aqueous surfaces, due to its peculiar molecular geometry that places the reactive hydroxylic −C(O)−OH group close to the interface.[19] Our findings are the more remarkable because in the gas-phase CH_2OO reacts with $(H_2O)_2$ and C_1−C_2 carboxylic acids at large rate constants, ∼10^{-11} and ∼10^{-10} cm^3 $molecule^{-1}$ s^{-1}, respectively.[20−22] The fact that CIs react with organic hydroxylic species in competition with water at air−aqueous interfaces bears directly on the mechanism of organic aerosol accretion and growth, because it amounts to a one-step polymerization process involving large molecules which has not been hitherto considered in chemical models of secondary organic aerosol formation.[23]

Here we report the first direct detection of intermediates and products from atmospherically relevant alcohol $C_nH_{2n+1}OH$ (n = 1−8) reactions with CIs generated on fresh surfaces of β-caryophyllene (β-C) and α-humulene (α-H) solutions in acetonitrile (AN):water (W) exposed to O_3(g) for ∼10 μs. Long-chain alcohols are ubiquitous surfactants found in a variety of atmospheric aerosol and sea-surface microlayers,[24−28] and therefore, their reactions with CIs could significantly contribute to the formation and augmentation of the chemical complexity of atmospheric particles and organic microfilms.

EXPERIMENTAL SECTION

The experimental setup is essentially the same as that reported elsewhere.[18,29] A brief description follows. We inject [sesquiterpene (β-C or α-H) + alcohol + NaCl] solutions in

Received: May 5, 2017
Revised: June 19, 2017
Published: June 21, 2017

DOI: 10.1021/acs.jpca.7b04272
J. Phys. Chem. A 2017, 121, 5175−5182

acetonitrile:water (AN:W = 4:1 = vol:vol) as microjets into the spraying chamber of an electrospray mass spectrometer (ES-MS, Agilent 6130 Quadrupole LC/MS Electrospray System at NIES, Japan) flushed with $N_2(g)$ at 1 atm, 298 K. We chose sesquiterpenes as in situ sources of CIs due to their high reactivity toward $O_3(g)$,[30] which makes them compatible with the short $\tau_R \sim 10$ μs contact times of our experiments.[31−33] We use a AN:W solvent mixture as surrogate of atmospheric aqueous organic aerosols because the composition of its interfacial layers is well characterized by both theory and experiments.[34,35] Microjets are exposed to an orthogonal $O_3(g)$ beam (Figure 1).

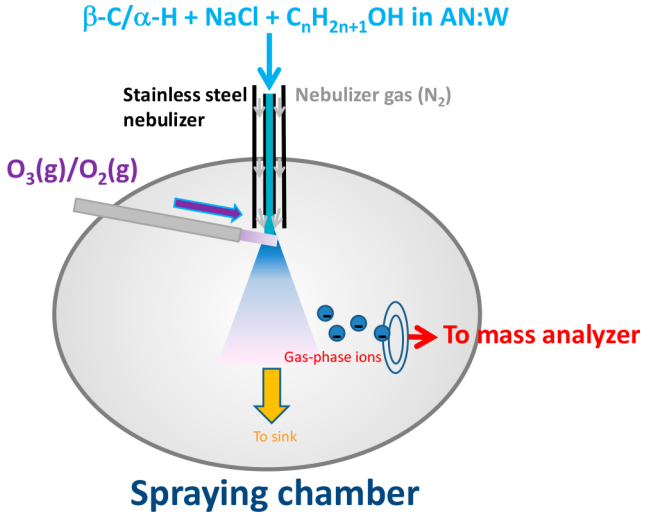

Figure 1. Schematic diagram of the experimental setup. β-C, α-H, AN, and W stand for β-caryophyllene, α-humulene, acetonitrile, and water, respectively.

AN:W solutions are pumped (at 100 μL min^{-1}) into the spraying chamber through a grounded stainless steel needle (100 μm bore) coaxial with a sheath issuing nebulizer $N_2(g)$ at high velocity v_g (~160 m s^{-1}).[36] The species detected by ES mass spectrometry are produced in $O_3(g)$ reactive collisions with the surface of the microjets as they emerge from the grounded nozzle.[31] Previous experiments in our laboratory have demonstrated that mass spectral signal intensities are proportional to interfacial ion populations.[31,32,36] We have shown that mass spectra (1) are not affected by the weak local electric fields at the tip of the grounded nozzle[37,38] and (2) correspond to species generated by reactions taking place in the outermost interfacial layers of the microjets.[29,31,32,39,40] The limited exposures of microjets to $O_3(g)$ during the short contact times of our experiments, $E = [O_3(g)] \times \tau_R \leq 2.4 \times 10^{11}$ molecules cm^{-3} s, enables us to monitor the earliest reactive events undergone by the CIs generated right at the liquid surface. Note that in our experiments the addition of NaCl lets us detect neutral species as negatively charged chloride adducts, which are unambiguously identified by the characteristic M/M + 2 = 3/1 signal ratios arising from natural abundance ^{35}Cl:^{37}Cl::0.75:0.25 isotopes. We verified that chloride is inert toward $O_3(g)$ under the present conditions.[41,42] Further experimental details can be found in previous publications.[18,29,32,33,36,40,43]

Ozone was generated by flowing ultrapure $O_2(g)$ (>99.999%) through a silent discharge ozonizer (KSQ-050, Kotohira, Japan) and quantified by online absorption spectrophotometry at 250 or 300 nm (Agilent 8453) prior to entering the reaction chamber. The reported $[O_3(g)]$ correspond to the concentrations sensed by the microjets, which are ~12 times smaller than the $[O_3(g)]$ determined by spectrophotometry due to dilution by the drying N_2 gas flow. Conditions in the present experiments: drying N_2 gas-flow rate, 12 L min^{-1}; drying N_2 gas temperature, 340 °C; inlet electric potential, +3.5 kV relative to ground; fragmentor polarization, 60 V. All solutions were prepared in Milli-Q water (resistivity ≥18.2 MΩ cm) and used within 48 h. β-Caryophyllene (≥98.5%, Sigma-Aldrich), α-humulene (≥96.0%, Sigma-Aldrich), methanol (≥99.9%, Sigma-Aldrich), ethanol (≥99.5%, Wako), 1-propanol (≥99.7%, Wako), 1-butanol (≥99.9%, Sigma-Aldrich), 1-pentanol (≥99%, Sigma-Aldrich), 1-hexanol (≥97%, Wako), 1-heptanol (≥98%, Wako), 1-octanol (≥99%, Sigma-Aldrich), *n*-octanoic acid (≥97%, Wako), acetonitrile (≥99.8%, Wako), D_2O (99.9 atom % D, Sigma-Aldrich), $H_2{}^{18}O$ (97%, Santa Cruz Isotope), and NaCl (≥99.999%, Sigma-Aldrich) were used as received.

RESULTS AND DISCUSSION

Figure 2 shows negative ion electrospray mass spectrum of [1 mM β-C + 0.2 mM NaCl + 100 mM 1-octanol] in AN:W (4:1 = vol:vol) microjets in the absence and presence of $O_3(g)$.

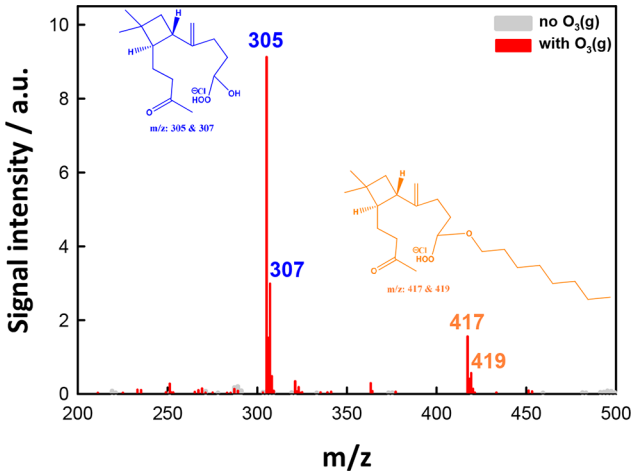

Figure 2. Negative ion electrospray mass spectra of [1 mM β-C + 0.2 mM NaCl + 100 mM 1-octanol] in AN:W (4:1 = vol:vol) microjets before (gray) and after (red) being exposed to $O_3(g)$ ($E = 4.1 \times 10^{10}$ molecules cm^{-3} s) in 1 atm $N_2(g)$ at 298 K. The *m*/*z* 305;307 and 417;419 signals correspond to chloride adducts of C_{15} α-hydroxy-hydroperoxides and C_{23} α-alkoxy-hydroperoxides, respectively. We show representative structures of possible isomers.

In the presence of $O_3(g)$, intense peaks appear at *m*/*z* 305;307 and 417;419 in M/M + 2 = 3/1 = ^{35}Cl/^{37}Cl ratios (Figure 2). We found that the ozonolysis of β-C on AN:W surfaces proceeds ~20 times faster than in the bulk liquid saturated with ozone,[30] and orders of magnitude faster than in the gas phase.[10,44] We confirmed that 1-octanol is inert toward $O_3(g)$ under the present conditions (Figure S1), in accordance with the negligibly small rate constant: $k_{O_3+1\text{-octanol}} \leq 0.8$ M^{-1} s^{-1} in bulk water.[45] The *m*/*z* 305;307 signals correspond to species resulting from the addition of O_3 (+48) to a β-C (MW = 204) endo C=C bond,[10,30] followed by the addition of H_2O (+18) and detected as chloride adducts: 305 (307) = 204 + 48 + 18 + 35 (37).[18] Our observation that (neutral) hydro-

DOI: 10.1021/acs.jpca.7b04272
J. Phys. Chem. A 2017, 121, 5175−5182

Scheme 1. Reaction Mechanism of β-Caryophyllene's Criegee Intermediate + n-Alkanols at Air−Aqueous Interfaces[a]

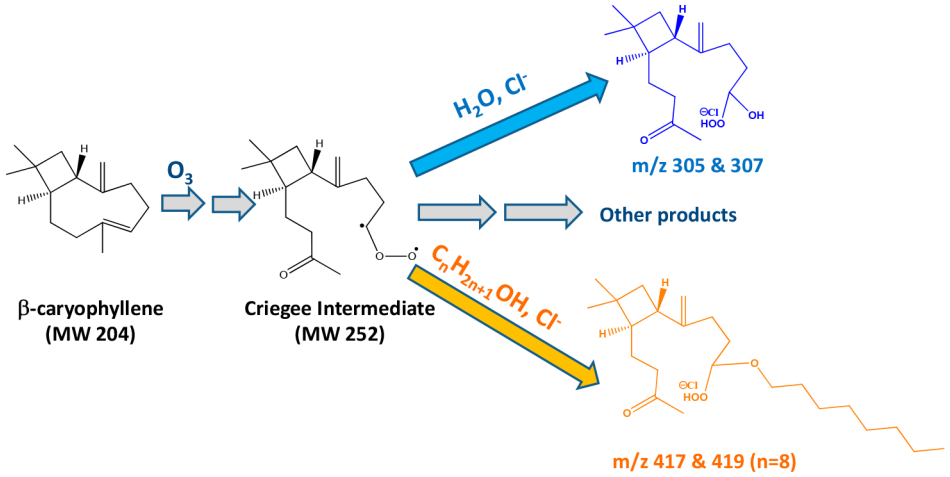

[a]Here we show representative structures among possible isomers.

peroxides form detectable chloride adducts is in line with the reported strong affinity of chloride for such species.[7,46,47] The m/z 417;419 signals correspond to the products of 1-octanol (MW = 130) addition to CIs: 417 (419) = 204 + 48 + 130 + 35 (37) (Scheme 1).

Thus, the m/z 417;419 signals are assigned to the α-alkoxy-hydroperoxides (C_{23} ethers) produced from CIs reactions with 1-octanol (Scheme 1). As mentioned above, we recently found that carboxylic acids R_n−COOH ($n \geq 4$) and a surface-active C_{10} keto-carboxylic acid at mM concentrations are able to compete with interfacial water molecules for the CIs derived from the ozonolysis of β-C or α-H on the surface of AN:W.[18,19] Here we find that 1-octanol also competes with interfacial water for CIs to generate a higher mass product (MW 382, detected as m/z 417 and 419) than the m/z = 305 α-hydroxy-hydroperoxides resulting from CIs reactions with $(H_2O)_n$. Similarly, in experiments involving shorter-chain alcohols at the same molar concentrations (Figures S2 and S3), we detect smaller signals at m/z = 204 + 48 + MW($C_nH_{2n+1}OH$, $4 \leq n \leq 7$) + 35(37) where signal intensity decreases as n decreases (see below). The formation of α-alkoxy-hydroperoxides from CIs reactions with alcohols is consistent with reports on ozonolyses in the gas and bulk liquid phases.[5,48−53] To our knowledge, this is the first-time report that α-alkoxy-hydroperoxides are produced from CIs reactions with alcohols in the presence of excess water at air−aqueous interfaces. Our results suggest the involvement of *interfacial* CIs chemistry in the prompt generation of molecular complexity on aqueous organic surfaces. Note that α-hydroxy-hydroperoxides and α-alkoxy-hydroperoxides are much less volatile than their precursors and can further extend this process into even less volatile species via free radical polymerizations upon thermal or photochemical O−OH bond dissociation,[54,55] or by addition to CIs.[3,23] Peaks at m/z 305;307 and 417;419 appear in the ozonolysis of both β-C and α-H in the presence of 1-octanol (Figure S4), thereby implying that CIs generated in situ will generally react with long-chain alcohols on aqueous organic surfaces.[56−59]

Additional evidence on the identity and mechanisms of formation of the observed products was obtained from negative ion electrospray mass spectrometry of [β-C + NaCl + 1-octanol] in AN:D_2O (Figure 3A) and AN:$H_2{}^{18}O$ (Figure 3B) microjets in the absence and presence of O_3(g).

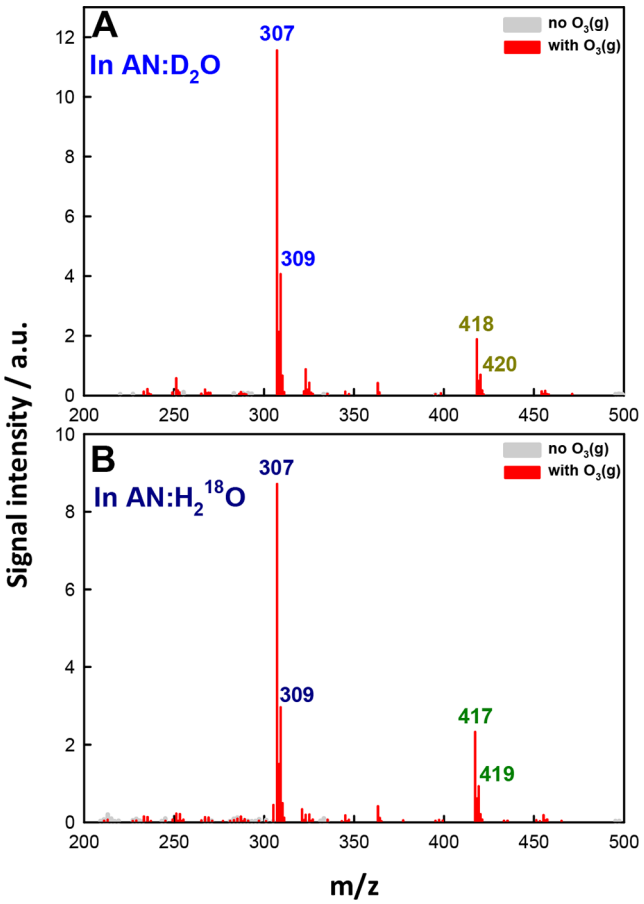

Figure 3. Negative ion electrospray mass spectra of (A) [1 mM β-C + 1 mM NaCl + 100 mM 1-octanol] in AN:D_2O (4:1 = vol:vol) microjets and (B) [1 mM β-C + 1.3 mM NaCl + 100 mM 1-octanol] in AN:$H_2{}^{18}O$ (4:1 = vol:vol) microjets before (gray) and after (red) being exposed to O_3(g) ($E = 1.4 \times 10^{11}$ molecules cm^{-3} s).

It is apparent that the m/z = 305;307 product signals shift by +2 mass units into 307;309 signals in both AN:D_2O and AN:$H_2{}^{18}O$ (Figure 3), in accordance with the formation of α-hydroxy-hydroperoxides possessing two exchangeable hydroxylic H atoms via the incorporation of a single water molecule (Scheme 1).[18] The observation that the m/z = 417;419 product

DOI: 10.1021/acs.jpca.7b04272
J. Phys. Chem. A 2017, 121, 5175−5182

signals shift by +1 mass unit into 418;420 signals in AN:D_2O (Figure 3A) but do not shift in AN:$H_2{}^{18}O$ (Figure 3B) is consistent with the formation of α-alkoxy-hydroperoxides (ethers) having a single exchangeable (OO)−H atom (Scheme 1).

Because the hydrophobic C_{23} ether products (MW 382, detected as m/z 417 and 419) still have one (in the case of β-C) and two (for α-H) C═C double bond(s), they would be further ozonolyzed, leading to higher O/C ratio products.[18] Ethers possessing hydroperoxide −OOH groups could propagate further polymerizations, as indicated above.[3,7,51,60] Such processes are deemed to contribute to the formation of the extremely low-volatility organic compounds (ELVOCs) detected in recent field studies of tropospheric aerosols.[23,53,61,62] Related high molecular weight species were also observed as major products in aerosols produced in the laboratory via α-pinene ozonolysis, and in aerosols collected over boreal forests.[50,53]

Figure 4 shows electrospray mass spectral signals acquired from [1 mM β-C + 0.2 mM NaCl + 100 mM 1-octanol] in AN:W (4:1 = vol:vol) microjets exposed to O_3(g) as functions of O_3(g) exposure (in 10^{10} molecules cm^{-3} s). Plotted m/z 417 signal intensities are 5-fold larger than actual values. The lines correspond to double exponential growth function regressions.

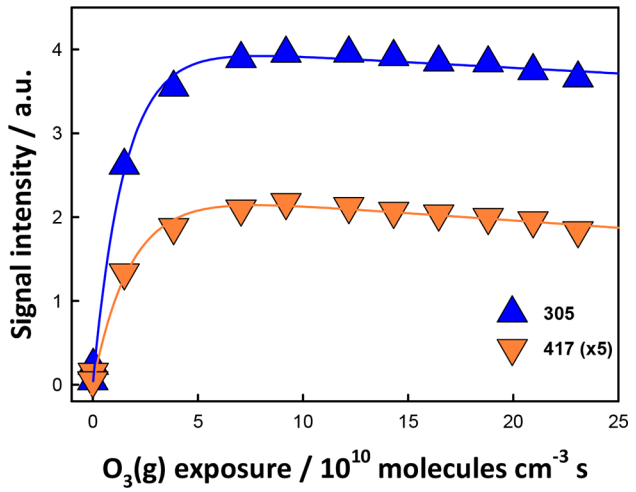

Figure 4. Mass spectral signal intensities from [1 mM β-C + 0.2 mM NaCl + 100 mM 1-octanol] in AN:W (4:1 = vol:vol) microjets exposed to O_3(g) as functions of O_3(g) exposure (in 10^{10} molecules cm^{-3} s). Plotted m/z 417 signal intensities are 5-fold larger than actual values. The lines correspond to double exponential growth function regressions.

AN:W (4:1) microjets exposed to gaseous O_3/O_2 mixtures as functions of O_3(g) exposure.

Both signals display nonzero initial slopes, as expected from early products generated within the first microseconds. The decline of m/z = 305 and 417 signals above $E \sim 1 \times 10^{11}$ molecules cm^{-3} s implies that at that point unsaturated products begin to compete for ozone with partially depleted reactant sesquiterpenes in interfacial layers.[18,63,64] This in turn implies that interfacial ozonolysis is faster than sesquiterpene diffusion from the bulk solution into interfacial layers. The key finding is that CIs react competitively with 1-octanol and interfacial $(H_2O)_n$ at significantly dissimilar bulk concentration ratios: [1-octanol]/[H_2O] = 100 mM/23 M ~ 4×10^{-3} (molar fraction of H_2O: mf_W = 0.42, in 4:1::AN:W).

We found that the reactivity of alcohols $C_nH_{2n+1}OH$ vs H_2O toward sesquiterpene CIs at the air−aqueous interface is a strongly increasing function of n. We quantified the competition between $C_nH_{2n+1}OH$ vs H_2O by the ratio of the mass spectral signal intensities: $m/z = X$ = 204 + 48 + MW($C_nH_{2n+1}OH$) + 35, of the C_{15+n} ether products of $C_nH_{2n+1}OH$ reactions with CIs vs over the m/z 305 signal intensity of the product of CIs reaction with H_2O: $X/305$ and $\ln(X/305)$ as a function of n at constant O_3(g) exposure (Figure 5).

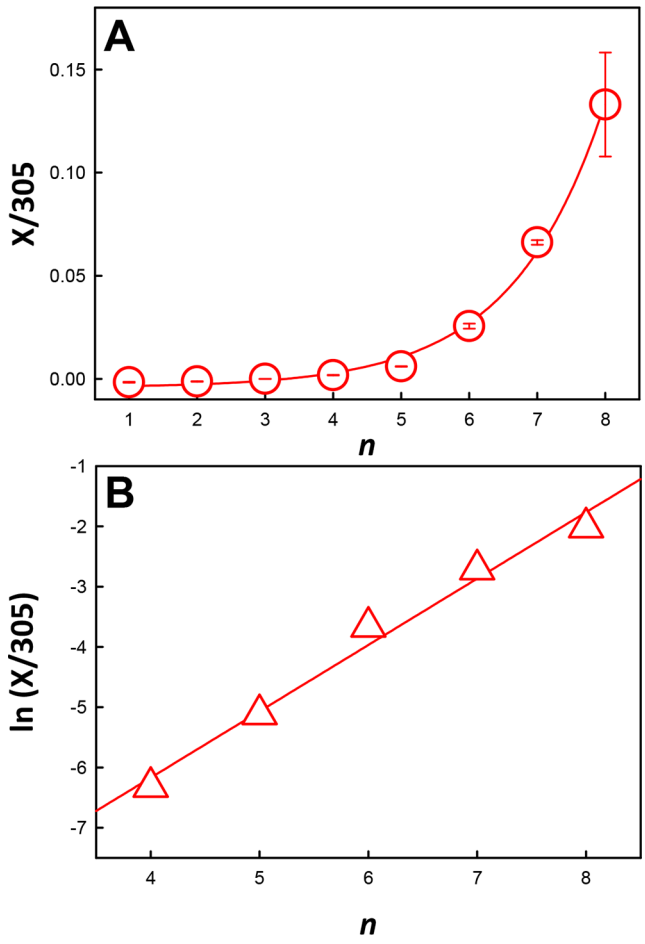

Figure 5. (A) $X/305$ ratio of signal intensities and (B) $\ln(X/305)$ from [1 mM β-C + 0.2 mM NaCl + 100 mM $C_nH_{2n+1}OH$] in AN:W (4:1 = vol:vol) microjets exposed to O_3(g) ($E \approx 1.4 \times 10^{11}$ molecules cm^{-3} s) as a function of n. X = 319, 333, 347, 361, 375, 389, 403, and 417 for n = 1, 2, 3, 4, 5, 6, 7, and 8, respectively. Error bars are derived from duplicate measurements. The line corresponds to a single exponential growth function regression.

The fact that the $X/305$ ratio is a strongly increasing function of n is consistent with the larger propensity of the longer alkyl chain alcohols for interfacial layers[65,66] and represents direct evidence that our experiments indeed probe interfacial events. The small $n \leq 3$ alcohols in fact did not generate detectable X signals (i.e., within background noise levels). Our results evoke a recent heterodyne-detected vibrational sum frequency generation (HD-VSFG) study, which revealed that whereas $C_nH_{2n+1}OH$ ($n < 4$) do not affect the structure and orientation of water at the air−water interface, the longer chain $C_nH_{2n+1}OH$ ($n > 4$) alcohols enhance H-bonding and force H_2O molecules to point their H atoms to the gas phase.[66] Recently, Walz et al. showed, by using X-ray photoelectron spectroscopy (XPS), that $C_nH_{2n+1}OH$ interfacial affinities exponentially increase as a function of n.[65] They reported free energies of $C_nH_{2n+1}OH$ adsorption to the air−water

DOI: 10.1021/acs.jpca.7b04272
J. Phys. Chem. A 2017, 121, 5175−5182

interface $\Delta G_{Ads}(n)$, which range from −15 to −19 kJ mol^{-1} for n = 4−6, respectively.[65] Similarly, we recently determined that the stabilization energy of R_n−COOH (n-alkanoic acids, $2 \leq n \leq 7$) at the air−water interface increases by ≈ 0.8 kJ mol^{-1} per additional −CH_2− group.[32]

However, the gas-phase acidity of alcohols also increases exponentially with n (see below).[67,68] In this regard, we found that the X/305 values in Figure 5 are ∼20 times smaller than those we previously reported for the corresponding products of CIs + R_n−COOH reactions on a molecular basis.[18] This effect is clearly apparent in Figure 6, which shows negative ion

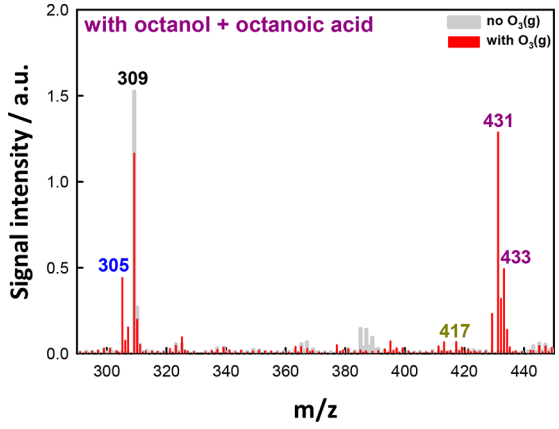

Figure 6. Negative ion electrospray mass spectra of [1 mM β-C + 0.2 mM NaCl + 100 mM 1-octanol +100 mM n-octanoic acid] in AN:W (4:1 = vol:vol) microjets before (gray) and after (red) being exposed to O_3(g) (E = 2.3 × 10^{11} molecules cm^{-3} s) in 1 atm N_2(g) at 298 K. The m/z 309 and 431;433 signals correspond to $Na(OA)_2^-$ and α-acyloxy-hydroperoxides (C_{23} esters) from the CIs + OA reaction, respectively.

electrospray mass spectra of [1 mM β-C + 0.2 mM NaCl + 100 mM 1-octanol +100 mM n-octanoic acid (OA, MW 144)] in AN:W (4:1 = vol:vol) microjets in the absence and presence of O_3(g).

The peaks at m/z 431 and 433 correspond to C_{23} esters produced from OA addition to CIs: 431 (433) = 204 + 48 + 144 + 35 (37).[18] Note that OA is inert toward O_3(g) in the absence of CIs.[40] The observation that signal intensities at m/z 417 (and 419) from 1-octanol are ∼25 times smaller than those at m/z 431 (and 433) from OA at [1-octanol] = [OA] = 100 mM reveals that 1-octanol is much less reactive than OA toward CIs, although both species are expected to have similar affinities for aqueous surfaces.[25,32,43,69,70] The C_{23} ethers and esters produced in each case, by having similar masses and structures (Scheme 1), are also expected to have similar interfacial affinities. Thus, the dissimilar mass spectral signal intensities in Figure 6 are bona fide indicators of the relative reactivities of n-alkanols vs n-alkanoic acids homologues toward CIs, and highlight the role of acidity in these processes. This finding is in line with gas-phase reaction rate constants of CIs + HCOOH/CH_3COOH, which approach collisionally controlled values: $k \geq 10^{-10}$ cm^3 molecule^{-1} s^{-1},[22] vs the much smaller values for CIs + methanol/2-propanol.[48,50,68] Tobias and Ziemann have reported that rate constants of gas-phase C_{13} CIs reactions with various species increase in the order: water < methanol < 2-propanol < formaldehyde < formic acid < heptanoic acid, over a 10^4 range.[68] Remarkably, the reactivity of CIs toward these hydroxylic compounds is not determined by their O−H bond dissociation energies but correlates with their gas-phase acidities, thereby suggesting polar transition states involving zwitterionic CIs.[68] Our results are in excellent accordance with Tobias and Ziemann's findings and strongly suggests that CIs reactions with hydroxylic compounds at the gas−aqueous interfaces proceed by a similar mechanism. This is confirmed by Figure 7, where we plotted ln(X/305) vs gas-

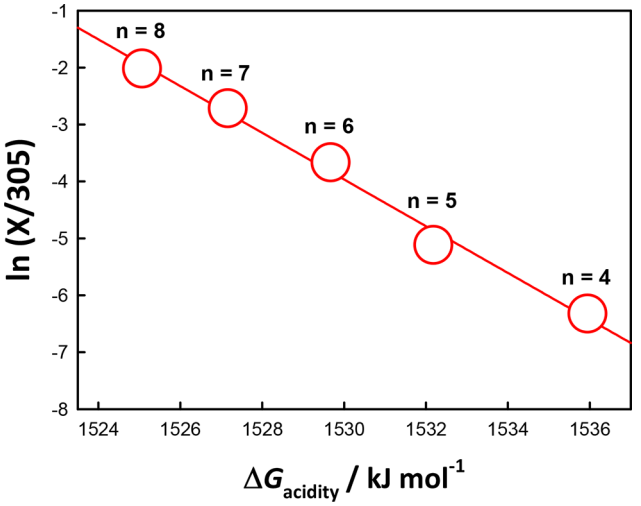

Figure 7. ln(X/305) plot from [1 mM β-C + 0.2 mM NaCl + 100 mM $C_nH_{2n+1}OH$ ($n \geq 4$)] in AN:W (4:1 = vol:vol) microjets exposed to O_3(g) ($E \approx 1.4 \times 10^{11}$ molecules cm^{-3} s) as a function of gas-phase $\Delta G_{acidity}$ values from ref 67.

phase $\Delta G_{acidity}$ values for $C_nH_{2n+1}OH$ ($n \geq 4$) alcohols. Recall that gas-phase acidity is the negative of the Gibbs free energy associated with deprotonation; i.e., the smaller absolute $\Delta G_{acidity}$ values correspond to the more acidic species. The exponential dependence of X with gas-phase $\Delta G_{acidity}$ values for $C_nH_{2n+1}OH$ (n = 1−8), which range from 1563 kJ mol^{-1} (n = 1) to 1525 kJ mol^{-1} (n = 8), is consistent with Tobias and Ziemann's findings and suggest similar reaction media in both cases, supporting our argument that the low water density at air−aqueous interfaces is a key factor underlying our observations.[68] From this perspective, the results of Figure 6 are consistent with the smaller gas-phase $\Delta G_{acidity}$ values for the n-alkanoic acids vs those for the n-alkanols: $\Delta G_{acidity}$ = 1429 kJ mol^{-1} (n = 1) to 1418 kJ mol^{-1} (n = 6) for R_n−COOH.[67,68,71]

Thus, the significant $\Delta G_{acidity}$ differences (≥100 kJ mol^{-1}) between alcohols vs carboxylic acids is what determines their relative reactivities toward CIs. Therefore, both the increasing interfacial affinities and acidities of the larger $C_nH_{2n+1}OH$ contribute to the strong X/305 vs n dependence in Figure 5.

Our experiments simulate a rapid ozonolysis process in which O_3(g) initially sticks to the surface of aqueous organic aerosols in the presence of unsaturated hydrocarbons and ubiquitous alcohols. We found that the heterogeneous ozonolysis of a solution of sesquiterpenes plus n-alkanols in AN:W leads to higher mass products, such as α-hydroxy-hydroperoxides and α-alkoxy-hydroperoxides (C_{15+n} ethers). Because long-chain alcohols are ubiquitous amphiphilic species found in atmospheric aerosols and sea-surface microlayers,[24−28] the interfacial chemistry on CIs involving alcohols would contribute to the growth/augmentation of atmospheric particles and to the formation of increasingly complex organic microfilms.

DOI: 10.1021/acs.jpca.7b04272
J. Phys. Chem. A 2017, 121, 5175−5182

CONCLUSION

Our experiments show that Criegee intermediates produced in the ozonolysis of sesquiterpenes in the interfacial layers of aqueous organic media react with long-chain $C_nH_{2n+1}OH$ ($n \geq 4$) alkanols to produce high-mass species (C_{15+n} ethers). Our results suggest that the reduced water concentration in interfacial layers relative to the bulk liquid makes amphiphilic components of aqueous organic aerosol competitive substrates for Criegee intermediates generated therein. The CI chemistry we observe on aqueous organic surfaces provides direct pathways to extremely low-volatility organic compounds (ELVOCs). From this perspective, our findings provide new insights into how to narrow down the mismatch between field observations and atmospheric model calculations regarding the evolution of chemical complexity in organic aerosols. We found that among C_n hydroxylic molecules, alcohols are significantly less reactive than carboxylic acids toward CIs and show that their reactivities depend on both interfacial affinities and gas-phase acidities.

ASSOCIATED CONTENT

Supporting Information

The Supporting Information is available free of charge on the ACS Publications website at DOI: 10.1021/acs.jpca.7b04272.

Additional experimental data (PDF)

AUTHOR INFORMATION

Corresponding Authors

*S.E. E-mail: enami.shinichi@nies.go.jp. Phone: +81-29-850-2770.

*A.J.C. E-mail: ajcoluss@caltech.edu. Phone: +1-626-395-6350.

ORCID

Shinichi Enami: 0000-0002-2790-7361

Author Contributions

S.E. designed and performed research. S.E. and A.J.C. analyzed data and wrote the paper.

Notes

The authors declare no competing financial interest.

ACKNOWLEDGMENTS

We acknowledge Drs. Satoshi Inomata, Akihiro Fushimi, and Kei Sato of NIES and Prof. Yosuke Sakamoto of Kyoto University. This work is partly supported by the research foundation for opto-science and technology, JSPS KAKENHI grant numbers 15H05328 and 15K12188.

REFERENCES

(1) Criegee, R. Mechanism of Ozonolysis. *Angew. Chem., Int. Ed. Engl.* **1975**, *14*, 745−752.

(2) Hatakeyama, S.; Akimoto, H. Reactions of Criegee Intermediates in the Gas-Phase. *Res. Chem. Intermed.* **1994**, *20*, 503−524.

(3) Sakamoto, Y.; Yajima, R.; Inomata, S.; Hirokawa, J. Water Vapour Effects on Secondary Organic Aerosol Formation in Isoprene Ozonolysis. *Phys. Chem. Chem. Phys.* **2017**, *19*, 3165−3175.

(4) Nguyen, T. B.; et al. Atmospheric Fates of Criegee Intermediates in the Ozonolysis of Isoprene. *Phys. Chem. Chem. Phys.* **2016**, *18*, 10241−10254.

(5) Yao, L.; Ma, Y.; Wang, L.; Zheng, J.; Khalizov, A.; Chen, M. D.; Zhou, Y. Y.; Qi, L.; Cui, F. P. Role of Stabilized Criegee Intermediate in Secondary Organic Aerosol Formation from the Ozonolysis of Alpha-Cedrene. *Atmos. Environ.* **2014**, *94*, 448−457.

(6) Taatjes, C. A.; Shallcross, D. E.; Percival, C. J. Research Frontiers in the Chemistry of Criegee Intermediates and Tropospheric Ozonolysis. *Phys. Chem. Chem. Phys.* **2014**, *16*, 1704−1718.

(7) Sakamoto, Y.; Inomata, S.; Hirokawa, J. Oligomerization Reaction of the Criegee Intermediate Leads to Secondary Organic Aerosol Formation in Ethylene Ozonolysis. *J. Phys. Chem. A* **2013**, *117*, 12912−12921.

(8) Mauldin, R. L., III; Berndt, T.; Sipila, M.; Paasonen, P.; Petaja, T.; Kim, S.; Kurten, T.; Stratmann, F.; Kerminen, V. M.; Kulmala, M. A New Atmospherically Relevant Oxidant of Sulphur Dioxide. *Nature* **2012**, *488*, 193−196.

(9) Beck, M.; Winterhalter, R.; Herrmann, F.; Moortgat, G. K. The Gas-Phase Ozonolysis of Alpha-Humulene. *Phys. Chem. Chem. Phys.* **2011**, *13*, 10970−11001.

(10) Winterhalter, R.; Herrmann, F.; Kanawati, B.; Nguyen, T. L.; Peeters, J.; Vereecken, L.; Moortgat, G. K. The Gas-Phase Ozonolysis of Beta-Caryophyllene ($C_{15}H_{24}$). Part I: An Experimental Study. *Phys. Chem. Chem. Phys.* **2009**, *11*, 4152−4172.

(11) Huang, H. L.; Chao, W.; Lin, J. J. M. Kinetics of a Criegee Intermediate That Would Survive High Humidity and May Oxidize Atmospheric SO_2. *Proc. Natl. Acad. Sci. U. S. A.* **2015**, *112*, 10857−10862.

(12) Matsuoka, K.; Sakamoto, Y.; Hama, T.; Kajii, Y.; Enami, S. Reactive Uptake of Gaseous Sesquiterpenes on Aqueous Surfaces. *J. Phys. Chem. A* **2017**, *121*, 810−818.

(13) Enami, S.; Mishra, H.; Hoffmann, M. R.; Colussi, A. J. Protonation and Oligomerization of Gaseous Isoprene on Mildly Acidic Surfaces: Implications for Atmospheric Chemistry. *J. Phys. Chem. A* **2012**, *116*, 6027−6032.

(14) Enami, S.; Hoffmann, M. R.; Colussi, A. J. Dry Deposition of Biogenic Terpenes via Cationic Oligomerization on Environmental Aqueous Surfaces. *J. Phys. Chem. Lett.* **2012**, *3*, 3102−3108.

(15) Spielmann, F.; Langebner, S.; Ghirardo, A.; Hansel, A.; Schnitzler, J. P.; Wohlfahrt, G.; Isoprene. and Alpha-Pinene Deposition to Grassland Mesocosms. *Plant Soil* **2017**, *410*, 313−322.

(16) Potier, E.; Loubet, B.; Durand, B.; Flura, D.; Bourdat-Deschamps, M.; Ciuraru, R.; Ogée, J. Chemical Reaction Rates of Ozone in Water Infusions of Wheat, Beech, Oak and Pine Leaves of Different Ages. *Atmos. Environ.* **2017**, *151*, 176−187.

(17) Zhu, C. Q.; Kumar, M.; Zhong, J.; Li, L.; Francisco, J. S.; Zeng, X. C. New Mechanistic Pathways for Criegee-Water Chemistry at the Air/Water Interface. *J. Am. Chem. Soc.* **2016**, *138*, 11164−11169.

(18) Enami, S.; Colussi, A. J. Criegee Chemistry on Aqueous Organic Surfaces. *J. Phys. Chem. Lett.* **2017**, *8*, 1615−1623.

(19) Enami, S.; Colussi, A. J. Efficient Scavenging of Criegee Intermediates on Water by Surface-Active Cis-Pinonic Acid. *Phys. Chem. Chem. Phys.* **2017**, DOI: 10.1039/C7CP03869K.

(20) Long, B.; Bao, J. L.; Truhlar, D. G. Atmospheric Chemistry of Criegee Intermediates: Unimolecular Reactions and Reactions with Water. *J. Am. Chem. Soc.* **2016**, *138*, 14409−14422.

(21) Lee, Y. P. Perspective: Spectroscopy and Kinetics of Small Gaseous Criegee Intermediates. *J. Chem. Phys.* **2015**, *143*, 020901.

(22) Welz, O.; et al. Rate Coefficients of C1 and C2 Criegee Intermediate Reactions with Formic and Acetic Acid near the Collision Limit: Direct Kinetics Measurements and Atmospheric Implications. *Angew. Chem., Int. Ed.* **2014**, *53*, 4547−4550.

(23) Barsanti, K. C.; Kroll, J. H.; Thornton, J. A. Formation of Low-Volatility Organic Compounds in the Atmosphere: Recent Advancements and Insights. *J. Phys. Chem. Lett.* **2017**, *8*, 1503−1511.

(24) Donaldson, D. J.; Vaida, V. The Influence of Organic Films at the Air−Aqueous Boundary on Atmospheric Processes. *Chem. Rev.* **2006**, *106*, 1445−1461.

(25) Gilman, J. B.; Eliason, T. L.; Fast, A.; Vaida, V. Selectivity and Stability of Organic Films at the Air-Aqueous Interface. *J. Colloid Interface Sci.* **2004**, *280*, 234−243.

(26) Fu, P. Q.; Kawamura, K.; Okuzawa, K.; Aggarwal, S. G.; Wang, G. H.; Kanaya, Y.; Wang, Z. F. Organic Molecular Compositions and Temporal Variations of Summertime Mountain Aerosols over Mt. Tai, North China Plain. *J. Geophys. Res.* **2008**, *113*, D19107.

DOI: 10.1021/acs.jpca.7b04272
J. Phys. Chem. A 2017, 121, 5175−5182

(27) Donaldson, D. J.; George, C. Sea-Surface Chemistry and Its Impact on the Marine Boundary Layer. *Environ. Sci. Technol.* **2012**, *46*, 10385−10389.
(28) Donaldson, D. J.; Valsaraj, K. T. Adsorption and Reaction of Trace Gas-Phase Organic Compounds on Atmospheric Water Film Surfaces: A Critical Review. *Environ. Sci. Technol.* **2010**, *44*, 865−873.
(29) Enami, S.; Sakamoto, Y.; Colussi, A. J. Fenton Chemistry at Aqueous Interfaces. *Proc. Natl. Acad. Sci. U. S. A.* **2014**, *111*, 623−628.
(30) Enami, S.; Hoffmann, M. R.; Colussi, A. J. Prompt Formation of Organic Acids in Pulse Ozonation of Terpenes on Aqueous Surfaces. *J. Phys. Chem. Lett.* **2010**, *1*, 2374−2379.
(31) Enami, S.; Colussi, A. J. Long-Range Hofmeister Effects of Anionic and Cationic Amphiphiles. *J. Phys. Chem. B* **2013**, *117*, 6276−6281.
(32) Enami, S.; Fujii, T.; Sakamoto, Y.; Hama, T.; Kajii, Y. Carboxylate Ion Availability at the Air-Water Interface. *J. Phys. Chem. A* **2016**, *120*, 9224−9234.
(33) Enami, S.; Hoffmann, M. R.; Colussi, A. J. Proton Availability at the Air/Water Interface. *J. Phys. Chem. Lett.* **2010**, *1*, 1599−1604.
(34) Perrine, K. A.; Van Spyk, M. H.; Margarella, A. M.; Winter, B.; Faubel, M.; Bluhm, H.; Hemminger, J. C. Characterization of the Acetonitrile Aqueous Solution/Vapor Interface by Liquid-Jet X-Ray Photoelectron Spectroscopy. *J. Phys. Chem. C* **2014**, *118*, 29378−29388.
(35) Makowski, M. J.; Stern, A. C.; Hemminger, J. C.; Tobias, D. J. Orientation and Structure of Acetonitrile in Water at the Liquid−Vapor Interface: A Molecular Dynamics Simulation Study. *J. Phys. Chem. C* **2016**, *120*, 17555−17563.
(36) Enami, S.; Colussi, A. J. Long-Range Specific Ion-Ion Interactions in Hydrogen-Bonded Liquid Films. *J. Chem. Phys.* **2013**, *138*, 184706.
(37) Enami, S.; Vecitis, C. D.; Cheng, J.; Hoffmann, M. R.; Colussi, A. J. Electrospray Mass Spectrometric Detection of Products and Short-Lived Intermediates in Aqueous Aerosol Microdroplets Exposed to a Reactive Gas. *J. Phys. Chem. A* **2007**, *111*, 13032−13037.
(38) Enami, S.; Hoffmann, M. R.; Colussi, A. J. How Phenol and Alpha-Tocopherol React with Ambient Ozone at Gas/Liquid Interfaces. *J. Phys. Chem. A* **2009**, *113*, 7002−7010.
(39) Enami, S.; Hoffmann, M. R.; Colussi, A. J. Extensive H-Atom Abstraction from Benzoate by OH-Radicals at the Air-Water Interface. *Phys. Chem. Chem. Phys.* **2016**, *18*, 31505−31512.
(40) Enami, S.; Hoffmann, M. R.; Colussi, A. J. In Situ Mass Spectrometric Detection of Interfacial Intermediates in the Oxidation of RCOOH(aq) by Gas-Phase OH-Radicals. *J. Phys. Chem. A* **2014**, *118*, 4130−4137.
(41) Hoigne, J.; Bader, H.; Haag, W. R.; Staehelin, J. Rate Constants of Reactions of Ozone with Organic and Inorganic-Compounds in Water 3. Inorganic-Compounds and Radicals. *Water Res.* **1985**, *19*, 993−1004.
(42) Enami, S.; Vecitis, C. D.; Cheng, J.; Hoffmann, M. R.; Colussi, A. J. Global Inorganic Source of Atmospheric Bromine. *J. Phys. Chem. A* **2007**, *111*, 8749−8752.
(43) Enami, S.; Sakamoto, Y. OH-Radical Oxidation of Surface-Active Cis-Pinonic Acid at the Air−Water Interface. *J. Phys. Chem. A* **2016**, *120*, 3578−3587.
(44) Ghalaieny, M.; Bacak, A.; McGillen, M.; Martin, D.; Knights, A. V.; O'Doherty, S.; Shallcross, D. E.; Percival, C. J. Determination of Gas-Phase Ozonolysis Rate Coefficients of a Number of Sesquiterpenes at Elevated Temperatures Using the Relative Rate Method. *Phys. Chem. Chem. Phys.* **2012**, *14*, 6596−6602.
(45) Hoigne, J.; Bader, H. Rate Constants of Reactions of Ozone with Organic and Inorganic-Compounds in Water − 1. Non-Dissociating Organic-Compounds. *Water Res.* **1983**, *17*, 173−183.
(46) Larson, J. W.; McMahon, T. B. Fluoride and Chloride Affinities of Main Group Oxides, Fluorides, Oxofluorides, and Alkyls. Quantitative Scales of Lewis Acidities from Ion Cyclotron Resonance Halide-Exchange Equilibria. *J. Am. Chem. Soc.* **1985**, *107*, 766−773.
(47) Bohringer, H.; Fahey, D. W.; Fehsenfeld, F. C.; Ferguson, E. E. Bond-Energies of the Molecules H_2O, SO_2, H_2O_2, and HCl to Various Atmospheric Negative-Ions. *J. Chem. Phys.* **1984**, *81*, 2805−2810.
(48) Neeb, P.; Horie, O.; Moortgat, G. K. Gas-Phase Ozonolysis of Ethene in the Presence of Hydroxylic Compounds. *Int. J. Chem. Kinet.* **1996**, *28*, 721−730.
(49) Witkowski, B.; Gierczak, T. Analysis of α-Acyloxyhydroperoxy Aldehydes with Electrospray Ionization−Tandem Mass Spectrometry (ESI-MSn). *J. Mass Spectrom.* **2013**, *48*, 79−88.
(50) Lee, S.; Kamens, R. M. Particle Nucleation from the Reaction of Alpha-Pinene and O_3. *Atmos. Environ.* **2005**, *39*, 6822−6832.
(51) Wang, M. Y.; Yao, L.; Zheng, J.; Wang, X. K.; Chen, J. M.; Yang, X.; Worsnop, D. R.; Donahue, N. M.; Wang, L. Reactions of Atmospheric Particulate Stabilized Criegee Intermediates Lead to High-Molecular-Weight Aerosol Components. *Environ. Sci. Technol.* **2016**, *50*, 5702−5710.
(52) Witkowski, B.; Gierczak, T. Early Stage Composition of SOA Produced by Alpha-Pinene/Ozone Reaction: Alpha-Acyloxyhydroperoxy Aldehydes and Acidic Dimers. *Atmos. Environ.* **2014**, *95*, 59−70.
(53) Kristensen, K.; Watne, Å. K.; Hammes, J.; Lutz, A.; Petäjä, T.; Hallquist, M.; Bilde, M.; Glasius, M. High-Molecular Weight Dimer Esters Are Major Products in Aerosols from α-Pinene Ozonolysis and the Boreal Forest. *Environ. Sci. Technol. Lett.* **2016**, *3*, 280−285.
(54) Tong, H.; Arangio, A. M.; Lakey, P. S. J.; Berkemeier, T.; Liu, F.; Kampf, C. J.; Brune, W. H.; Pöschl, U.; Shiraiwa, M. Hydroxyl Radicals from Secondary Organic Aerosol Decomposition in Water. *Atmos. Chem. Phys.* **2016**, *16*, 1761−1771.
(55) Vidrio, E.; Phuah, C. H.; Dillner, A. M.; Anastasio, C. Generation of Hydroxyl Radicals from Ambient Fine Particles in a Surrogate Lung Fluid Solution. *Environ. Sci. Technol.* **2009**, *43*, 922−927.
(56) Ruehl, C. R.; Wilson, K. R. Surface Organic Mono Layers Control the Hygroscopic Growth of Submicrometer Particles at High Relative Humidity. *J. Phys. Chem. A* **2014**, *118*, 3952−3966.
(57) Müller, L.; Reinnig, M. C.; Naumann, K. H.; Saathoff, H.; Mentel, T. F.; Donahue, N. M.; Hoffmann, T. Formation of 3-Methyl-1,2,3-Butanetricarboxylic Acid via Gas Phase Oxidation of Pinonic Acid - A Mass Spectrometric Study of SOA Aging. *Atmos. Chem. Phys.* **2012**, *12*, 1483−1496.
(58) Cheng, Y.; Brook, J. R.; Li, S. M.; Leithead, A. Seasonal Variation in the Biogenic Secondary Organic Aerosol Tracer Cis-Pinonic Acid: Enhancement Due to Emissions from Regional and Local Biomass Burning. *Atmos. Environ.* **2011**, *45*, 7105−7112.
(59) Zhang, Y. Y.; Muller, L.; Winterhalter, R.; Moortgat, G. K.; Hoffmann, T.; Poschl, U. Seasonal Cycle and Temperature Dependence of Pinene Oxidation Products, Dicarboxylic Acids and Nitrophenols in Fine and Coarse Air Particulate Matter. *Atmos. Chem. Phys.* **2010**, *10*, 7859−7873.
(60) Riva, M.; Budisulistiorini, S. H.; Zhang, Z.; Gold, A.; Thornton, J. A.; Turpin, B. J.; Surratt, J. D. Multiphase Reactivity of Gaseous Hydroperoxide Oligomers Produced from Isoprene Ozonolysis in the Presence of Acidified Aerosols. *Atmos. Environ.* **2017**, *152*, 314−322.
(61) Ehn, M.; et al. A Large Source of Low-Volatility Secondary Organic Aerosol. *Nature* **2014**, *506*, 476−479.
(62) Riccobono, F.; et al. Oxidation Products of Biogenic Emissions Contribute to Nucleation of Atmospheric Particles. *Science* **2014**, *344*, 717−721.
(63) Kjaergaard, H. G.; Kurten, T.; Nielsen, L. B.; Jorgensen, S.; Wennberg, P. O. Criegee Intermediates React with Ozone. *J. Phys. Chem. Lett.* **2013**, *4*, 2525−2529.
(64) Vereecken, L.; Harder, H.; Novelli, A. The Reactions of Criegee Intermediates with Alkenes, Ozone, and Carbonyl Oxides. *Phys. Chem. Chem. Phys.* **2014**, *16*, 4039−4049.
(65) Walz, M. M.; Werner, J.; Ekholm, V.; Prisle, N. L.; Ohrwall, G.; Bjorneholm, O. Alcohols at the Aqueous Surface: Chain Length and Isomer Effects. *Phys. Chem. Chem. Phys.* **2016**, *18*, 6648−6656.
(66) Mondal, J. A.; Namboodiri, V.; Mathi, P.; Singh, A. K. Alkyl Chain Length Dependent Structural and Orientational Trans-

DOI: 10.1021/acs.jpca.7b04272
J. Phys. Chem. A 2017, 121, 5175−5182

formations of Water at Alcohol−Water Interfaces and Its Relevance to Atmospheric Aerosols. *J. Phys. Chem. Lett.* **2017**, *8*, 1637−1644.
(67) Boand, G.; Houriet, R.; Gaumann, T. Gas-Phase Acidity of Aliphatic-Alcohols. *J. Am. Chem. Soc.* **1983**, *105*, 2203−2206.
(68) Tobias, H. J.; Ziemann, P. J. Kinetics of the Gas-Phase Reactions of Alcohols, Aldehydes, Carboxylic Acids, and Water with the C13 Stabilized Criegee Intermediate Formed from Ozonolysis of 1-Tetradecene. *J. Phys. Chem. A* **2001**, *105*, 6129−6135.
(69) Donaldson, D. J.; Anderson, D. Adsorption of Atmospheric Gases at the Air-Water Interface. 2. C-1-C-4 Alcohols, Acids, and Acetone. *J. Phys. Chem. A* **1999**, *103*, 871−876.
(70) Houriez, C.; Meot-Ner, M.; Masella, M. Simulated Solvation of Organic Ions II: Study of Linear Alkylated Carboxylate Ions in Water Nanodrops and in Liquid Water. Propensity for Air/Water Interface and Convergence to Bulk Solvation Properties. *J. Phys. Chem. B* **2015**, *119*, 12094−12107.
(71) Caldwell, G.; Renneboog, R.; Kebarle, P. Gas-Phase Acidities of Aliphatic Carboxylic-Acids, Based on Measurements of Proton-Transfer Equilibria. *Can. J. Chem.* **1989**, *67*, 611−618.

DOI: 10.1021/acs.jpca.7b04272
J. Phys. Chem. A 2017, 121, 5175−5182